Bridging Rh–Fe Borataaminocarbyne Complexes Formed by Intramolecular Isonitrile–Borane Coordination

*Bradley E. Cowie and David J. H. Emslie**

Department of Chemistry and Chemical Biology, McMaster University, 1280 Main Street West, Hamilton, Ontario, L8S 4M1, Canada.

ABSTRACT

Reaction of [(TXPB)Rh(μ-CO)$_2$Fe(CO)Cp] (**1**; TXPB = 2,7-di-*tert*-butyl-5-diphenylboryl-4-diphenylphosphino-9,9-dimethylthioxanthene) with both aryl- and alkyl-isonitriles formed [(TXPB)Rh(μ-CO)(μ-CNR)Fe(CO)Cp] {R = C$_6$H$_4$Cl-*p* (**2**), Xyl (**3**) and ^{n}Bu (**4**); Xyl = 2,6-dimethylphenyl} in which the CNRBR$_3$ unit is best described as a borataaminocarbyne ligand with single bonds between carbon and nitrogen and between nitrogen and boron. The carbon atom of the borataaminocarbyne ligand is doubly bound to iron and singly bound to rhodium. For comparison, borane-free [(TXPH)Rh(μ-CO)$_2$Fe(CO)Cp] (**5**; TXPH = 2,7-di-*tert*-butyl-4-diphenylphosphino-9,9-dimethylthioxanthene) was prepared from [(TXPH)RhCl(CO)] and K[CpFe(CO)$_2$], and reaction of **5** with either 1 or 2 equivalents of CNC$_6$H$_4$Cl-*p* afforded [(TXPH)Rh(CO)(μ-CNC$_6$H$_4$Cl-*p*)$_2$Fe(CO)Cp] (**6**), which contains two μ-isonitrile ligands and two terminal carbonyl ligands; one bound to iron and the other to rhodium. The C–N stretching frequency for **6** is 124 cm^{-1} higher than that for the TXPB CNC$_6$H$_4$Cl-*p* complex **2**, and the Rh–(μ-CNR), Fe–(μ-CNR) and C–N distances are notably longer than those in **2**.

Introduction

In 2006 and 2008, we reported the first examples of transition metal complexes in which a triarylborane is η^3*(BCC)*-coordinated[1] to a metal center; [(TXPB)Rh(μ-CO)$_2$Fe(CO)Cp] (**1**),[2] [Pd(TXPB)] and [Ni(TXPB)][3] (Figure 1; TXPB = 2,7-di-*tert*-butyl-5-diphenylboryl-4-diphenylphosphino-9,9-dimethylthioxanthene).[4] The borane in these complexes is incorporated into a rigid phosphine-thioether-borane ambiphilic[5] ligand (TXPB), and while a variety of reactions have been carried out to probe the potential for these borane complexes to engage in cooperative substrate binding and reactivity, most resulted in displacement of both the thioether donor and the borane from the metal, or displacement of the entire TXPB ligand from the metal. For example, reaction of [Pd(TXPB)] with CO yielded free TXPB, and reaction of [Pd(TXPB)] with dvds (1,3-divinyltetramethydisiloxane) yielded [(κ^1*(P)*-TXPB)Pd(η^2:η^2-dvds)] in which TXPB acts as a monodentate phosphine ligand (Figure 1).[3] One of the few more productive reactions was the reaction of [Pd(TXPB)] with dba (*trans*,*trans*-dibenzylideneacetone) to form [Pd(dba)(TXPB)] (Figure 1), which can be described as a zwitterionic palladium(II) boratoxyallyl complex.[4] Herein, we describe the reactions of **1** with isonitriles to yield products in which both P- and S-coordination is maintained, and boron is bound to the nitrogen atom of the CNR unit in the product. Spectroscopic and structural studies to ascertain the most appropriate bonding description for the resulting CNRBR$_3$ ligand are described, along with attempts to prepare a borane-free analogue of these complexes using the TXPH (2,7-di-*tert*-butyl-4-diphenylphosphino-9,9-dimethylthioxanthene) ligand.[6] In light of the fact that this work deals with isonitrile ligand–borane coordination, a brief discussion of the canonical forms relevant to CNR, CNR(LA) (LA = Lewis acid) and related CNR$_2$ ligands is provided below.

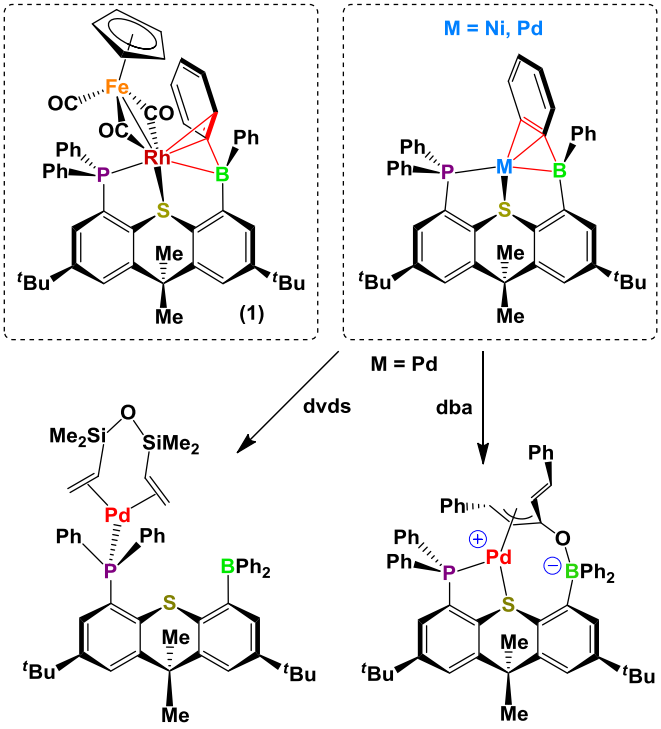

Figure 1. TXPB complexes in which the borane is η^3*(BCC)*-coordinated to the metal (enclosed in dashed boxes), and reactions of [Pd(TXPB)] with dvds and dba.

Three canonical forms can be used to describe CNR ligands (Figure 2); form I is most prevalent in terminal CNR complexes, form II tends to dominate for bridging CNR complexes, and form III is generally not considered to play an important role.[7,8,9] However, coordination of a Lewis acid at the nitrogen atom of a bridging isonitrile ligand has in a few cases resulted in complexes with long C–N bonds and/or particularly low C–N stretching frequencies; see **A,**[10] **B**[11] and **C**[12-13] in Figure 3. These complexes are essentially Lewis acid adducts of canonical form III, and **B** is to the best of our knowledge the only example of a borataaminocarbyne complex; it is certainly the only crystallographically characterized example.

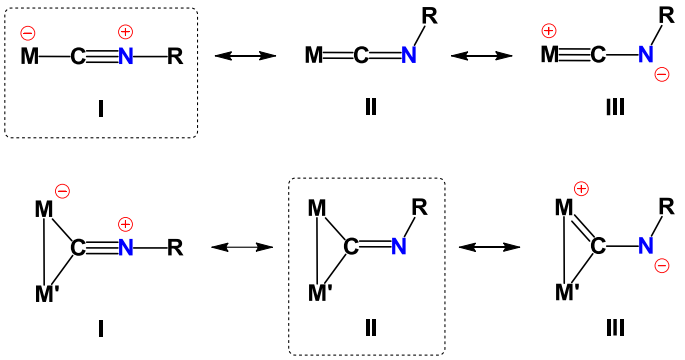

Figure 2. Three canonical forms for terminal and bridging isonitrile ligands. In each case, dashed lines enclose the canonical form that typically play a dominant role.

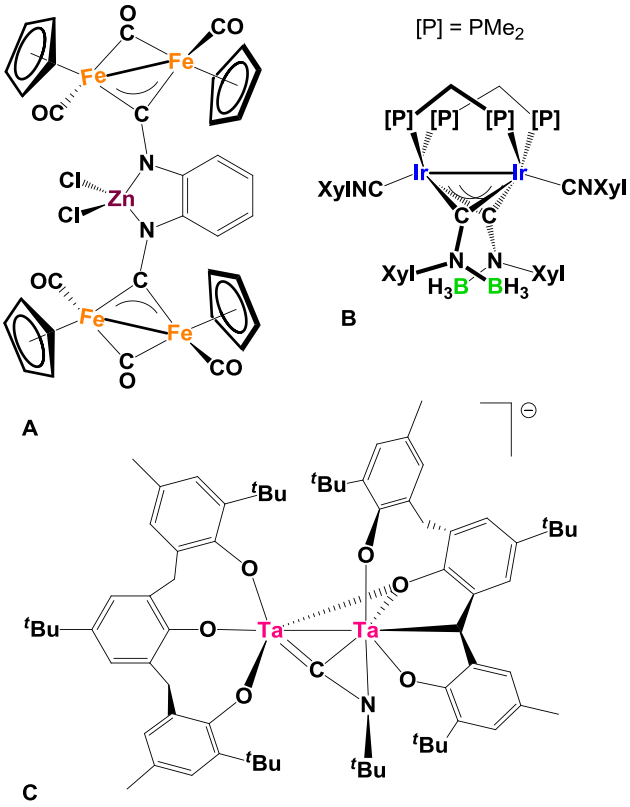

Figure 3. Literature examples of μ-C–NR(LA) complexes where LA is a Lewis acid (LA = $ZnCl_2$ in **A**, BH_3 in **B**, and TaR_x in **C**).[10,11,1213]

The Lewis acid substituted aminocarbyne [CNR(LA)] complexes described above are related to aminocarbyne (CNR_2) complexes, in which an alkyl cation or a proton can be considered, conceptually,

to play the role of the Lewis acid (see Figure 4 for examples).[14-17] Naturally, aminocarbyne ligands represent just one of two possible canonical forms for a CNR_2 ligand. The other canonical form is that of an azavinylidene ligand,[18] which is analogous to a borane-coordinated bent isonitrile ligand (a borataazavinylidene) in the same way that an aminocarbyne ligand is analogous to a borataaminocarbyne ligand (Figure 5).

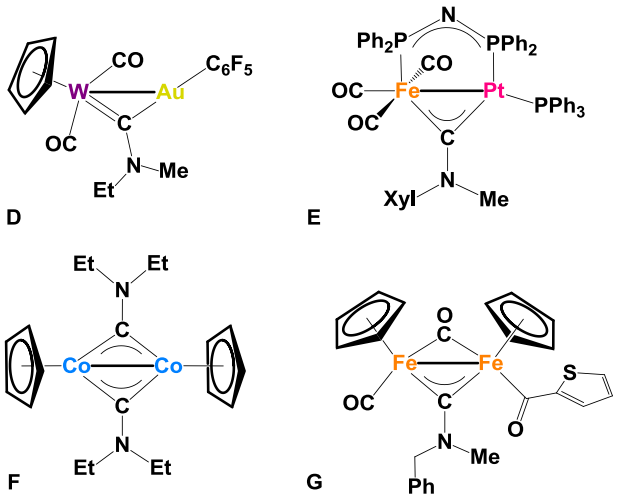

Figure 4. Literature examples of late transition metal μ-aminocarbyne complexes (**D-G**).[14-17]

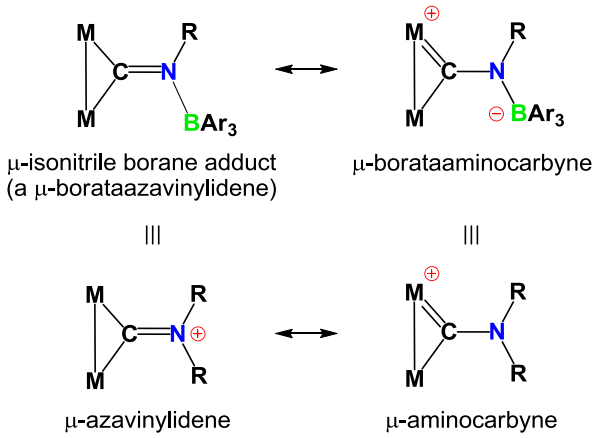

Figure 5. Canonical forms for a bridging $CNR(BR_3)$ ligand, and the analogous canonical forms for a CNR_2 ligand. For directly analogous $CNR(BR_3)$ and CNR_2 complexes, the overall charge on the CNR_2 complex would be more positive by one unit.

Results and Discussion

Reactivity of [(TXPB)Rh(μ-CO)$_2$Fe(CO)Cp] with Isonitriles: Reaction of olive-green [(TXPB)Rh(μ-CO)$_2$Fe(CO)Cp] (**1**; TXPB = 2,7-di-*tert*-butyl-5-diphenylboryl-4-diphenylphosphino-9,9-dimethylthioxanthene)[2] with 1 equivalent of CNC$_6$H$_4$Cl-*p*, CNXyl and CN^{n}Bu yielded dark purple or dark red [(TXPB)Rh(μ-CO)(μ-CNR)Fe(CO)Cp] {R = C$_6$H$_4$Cl-*p* (**2**), Xyl (**3**) and ^{n}Bu (**4**); Xyl = 2,6-dimethylphenyl}. By contrast, reaction of **1** with 1 equivalent of more electron donating and sterically encumbered ^{t}BuNC afforded the ^{t}BuNC adduct of TXPB[19] accompanied by unidentified metal complexes (Scheme 1). The borane in starting complex **1** was η^3*(BCC)*-coordinated to rhodium, whereas the borane in **2-4** is bound solely to the nitrogen atom of the bridging CNR ligand.

Complexes **2-4** gave rise to a doublet at 44-47 ppm in their ^{31}P NMR spectra ($^1J_{P,Rh}$ = 148-151 Hz), and a broad ^{11}B NMR signal between 2 and 4 ppm, indicative of 4-coordinate boron. Consistent with the structure depicted in Scheme 1, both *B*-phenyl rings are inequivalent in the ^{1}H and ^{13}C NMR spectra, and all positions on one of the *B*-phenyl rings became inequivalent below 0 °C.[19] However, ^{13}C–^{103}Rh or ^{1}H–^{103}Rh coupling was not observed for any of the *B*-phenyl signals down to –90 °C on a 500 MHz NMR spectrometer, indicating that the η^2-arene interaction observed in the solid state structures of **2-4** (*vide infra*) is labile in solution. In the ^{13}C NMR spectra of **2-4**, the CO ligand on iron is located at 215-216 ppm, and the bridging CO ligand appears as a doublet of doublets at 241-243 ppm ($^1J_{C,Rh}$ 60 Hz, $^2J_{C,P}$ 10-11 Hz). The *C*NR signal appears as a doublet of doublets at 312 ppm (compounds **2** and **3**) or 304 ppm (compound **4**) with a $^1J_{C,Rh}$ coupling of 51-53 Hz and a $^2J_{C,P}$ coupling of 23-24 Hz. This *C*NR signal is at unusually high frequency for a bridging isonitrile ligand (typically <250 ppm),[7,8] but is in the range for an aminocarbyne complex (~ 200-350 ppm). In addition, the C–N stretching frequencies for complexes **2-4** lie between 1571 and 1521 cm^{-1}, which is significantly lower than is typically observed for a μ-isonitrile complex (>1600 cm^{-1}),[7,9] but is in line with an aminocarbyne complex (most often 1500-1600 cm^{-1}),[18] indicating that a borataaminocarbyne bonding description is

appropriate for **2**-**4**. For comparison, the C–N stretching frequencies for the CNR(LA) ligands in complexes **A** and **B** in Figure 3 are 1534 and 1514 cm^{-1} (**A**; LA = $ZnCl_2$),[10] and 1520 and 1502 cm^{-1} (**B**; LA = BH_3).[11]

Scheme 1. Reaction of TXPB complex **1** with isonitriles.

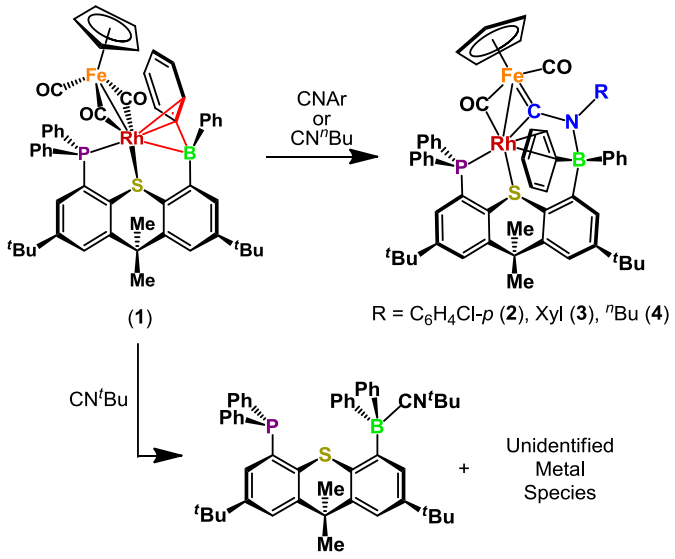

X-ray quality crystals of **2**·2hexane, **3**·5toluene and **4**·2hexane were grown from hydrocarbon solvents at –30 °C. The structures of **2** and **4** are provided in Figure 6, while the structure of **3** is located in the supporting information. Key bond lengths and angles are summarized in Table 1. All three structures share the same general features; the TXPB ligand is κ^2*(PS)*-coordinated to rhodium, the Rh–Fe distance is 2.594–2.606 Å, one CO and one CNR group bridge between rhodium and the Fe(CO)(η^5-Cp) group, boron is coordinated to the nitrogen atom of the bridging CNR unit, and one *B*-phenyl ring is η^2-coordinated to rhodium.

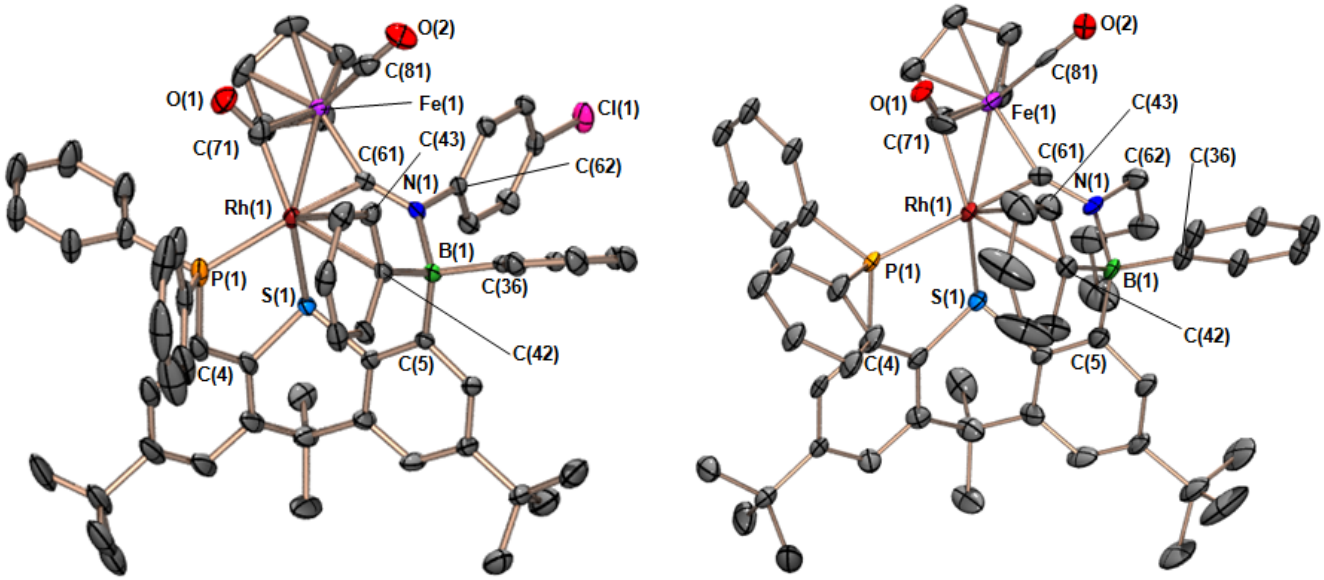

Figure 6. X-ray crystal structures for complexes **2**·2hexane and **4**·2hexane. Hydrogen atoms and lattice solvent are omitted for clarity. Ellipsoids are set to 50 %. Positional and/or rotational disorder was found in both structures; for clarity only one orientation of the disordered groups is displayed.

Complex number	**2**	**3**	**4**	**5**	**6**
Multidentate Ligand	TXPB	TXPB	TXPB	TXPH	TXPH
Bridging Ligands	(CO)(CNC_6H_4Cl-*p*)	(CO)(CNXyl)	(CO)(CN^nBu)	$(CO)_2$	$(CNC_6H_4Cl\text{-}p)_2$
Lattice Solvent	2 hexane	5 toluene	2 hexane	2 $C_2H_4Cl_2$-1,2	CH_2Cl_2
Rh(1)–P(1)	2.333(1)	2.321(1)	2.339(1)	2.290(2)	2.330(1)
Rh(1)–S(1)	2.426(1)	2.403(2)	2.386(1)	2.355(2)	2.441(1)
Rh(1)–C(61)	1.968(3)	1.981(5)	1.975(5)	2.055(8)	2.051(5)
Rh(1)–C(71)	1.912(3)	1.906(7)	1.908(6)	1.947(7)	2.021(5)
Rh(1)–C(82)	n/a	n/a	n/a	n/a	1.926(6)
Rh(1)–Fe(1)	2.606(1)	2.597(1)	2.601(1)	2.594(1)	2.631(1)
Fe(1)–C(61)	1.833(3)	1.864(6)	1.851(5)	1.909(8)	1.908(5)
Fe(1)–C(71)	2.116(3)	2.088(5)	2.090(7)	1.981(7)	1.943(5)
Fe(1)–C(81)	1.760(4)	1.756(6)	1.748(6)	1.768(9)	1.755(6)
C(61)–N(1)	1.284(3)	1.298(7)	1.294(6)	n/a	1.239(6)
C(71)–N(2)	n/a	n/a	n/a	n/a	1.246(7)
N(1)–B(1)	1.641(4)	1.660(8)	1.654(7)	n/a	n/a
C(61)–N(1)–B(1)	119.1(2)	119.1(4)	119.1(4)	n/a	n/a
C(61)–N(1)–C(62)	117.5(2)	114.0(5)	118.4(4)	n/a	126.8(4)
C(62)–N(1)–B(1)	123.4(2)	126.8(4)	122.4(4)	n/a	n/a
C(71)–N(2)–C(72)	n/a	n/a	n/a	n/a	132.7(4)
C(36)–B(1)–C(5)	111.9(2)	111.2(5)	111.0(8), 118.1(8)[a]	n/a	n/a
C(36)–B(1)–C(42)	108.7(2)	111.8(5)	114.7(7), 103.9(7)[a]	n/a	n/a
C(42)–B(1)–C(5)	110.5(2)	108.4(4)	109.7(4)	n/a	n/a

(a) One of the *B*-phenyl rings in **4**·2hexane (C36-C41) was disordered over two positions, therefore values have been tabulated for both orientations.

Table 1. Selected bond lengths (Å) and angles (°) for TXPB and TXPH complexes **2-6**.

The Fe–C(61) bonds in **2**–**4** are 1.833(3), 1.864(6) and 1.851(5) Å, respectively, falling well within the range for complexes with an Fe–C double bond. For example, the Fe–C_{CR2} distances in terminal carbene complexes [Cp{$CO_2Zr(NR_2)_3$}(CO)Fe=CR_2] (CR_2 = 1,2-diphenylcyclopropenylidene)[20] and [Cp($SSiPh_3$)(CO)Fe=$CH(NMe_2)$][21] are 1.860(5) and 1.889(2) Å, whereas the Fe–C_{CNR} and Fe–C_{CCR2} bonds in [{$CpFe(CO)\}_2$(μ-CO)(μ-CNPh)][22] (a bent isonitrile complex) and [{$CpFe(CO)\}_2$(μ-CO)(μ-C=CH^iPr)][23] are 1.915(3)-1.969(8) Å. The Rh–C(61) bonds in **2**–**4** are 1.968(3), 1.981(5) and 1.975(5) Å, respectively, indicative of a Rh–C single bond; the Rh–C_{CR2} double bonds in [Cp(CO)Rh=CPh_2][24] and *trans*-[$Cl(Sb^iPr_3)_2$Rh=CPh_2][25] are 1.906(3) and 1.863(4) Å, while the Rh–C_{CNR} and Rh–C_{CCR2} single bonds in [$(Cp^*Rh)_2$(μ-$CNXyl)_2$],[26] [{$Cp^*Rh(CO)\}_2$(μ-C=CMe_2)][27] and [{Rh(CO)(PCy_3)}$_2$(μ-O_2CMe)(μ-C=CPh_2)][28] range from 1.967(6) to 2.043(1) Å. Consistent with the low C–N stretching frequencies for **2**-**4** (*vide supra*), the C–N bonds in **2**–**4** are notably long at 1.284(3), 1.298(7) and 1.294(6) Å, respectively. For comparison, the C–N distances in the μ-isonitrile complexes described above are 1.229(4) and 1.234(8) Å, whereas the C–N bonds in μ-aminocarbyne complexes **D-G** (Figure 4) are 1.29(2),[14] 1.296(6),[15] 1.312(4)[16] and 1.303(5)[17] Å, respectively, and the C–N bond in borataaminocarbyne complex **B** (Figure 3) is 1.34(2) Å.[11] Taken together, these structural data point to a μ-borataaminocarbyne bonding description for the $CNRBR_3$ unit in **2**–**4**; one in which the carbyne carbon is doubly bound to iron and singly bound to rhodium.

The only features of **2**–**4** that are at first glance incommensurate with a μ-borataaminocarbyne bonding description are the long B–N bond lengths of 1.641(4), 1.660(8) and 1.654(7) Å, respectively. These distances are more in keeping with the B–N distances in neutral Lewis base–borane adducts such as MePhC=N(CH_2Ph)–B(C_6F_5)$_3$ [1.630(6) and 1.658(6) Å][29] and 1-phenylimidazole–BPh_3 [1.630(3) Å].[29] The elongated B–N bonds in **2**–**4** can likely be explained on the basis of steric arguments. The B–

N distance in **B** (Figure 3) is 1.59(3) Å,[11] but meaningful comparison is impossible given the large standard deviation on this measurement.

Synthesis of [(TXPH)Rh(μ-CO)$_2$Fe(CO)Cp] and Reactivity with CNC$_6$H$_4$Cl-*p*: As an alternative means to probe the effects of boron–nitrogen coordination in TXPB complexes **2**-**4**, a borane-free analogue of **2** was targeted. Reaction of [RhCl(CO)(TXPH)] (TXPH = 2,7-di-*tert*-butyl-4-diphenylphosphino-9,9-dimethylthioxanthene)[6] with K[CpFe(CO)$_2$] provided the borane-free analogue of **1**, orange-brown [(TXPH)Rh(μ-CO)$_2$Fe(CO)Cp] (**5**). Subsequent reaction of **5** with 1 equivalent of CNC$_6$H$_4$Cl-*p* afforded [(TXPH)Rh(CO)(μ-CNC$_6$H$_4$Cl-*p*)$_2$Fe(CO)Cp] (**6**) and remaining **5**, and addition of a second equivalent of CNC$_6$H$_4$Cl-*p* pushed the reaction to completion. Unlike TXPB complex **2**, TXPH complex **6** contains two bridging isonitrile ligands. Furthermore, while **2** features an η^2-interaction between rhodium and one of the phenyl rings on boron, and a terminal CO ligand resides on the rhodium centre in **6**. The divergent reactivity of **1** and **5** with CNC$_6$H$_4$Cl-*p* can be ascribed either to the increased steric bulk of TXPB relative to TXPH, or to differences between the electronic structures of **2** and the undetected TXPH analogue of **2** as a result of boron–nitrogen coordination in the former (leading to a μ-borataaminocarbyne complex).

Scheme 2. Synthesis of TXPH complexes **5** and **6**.

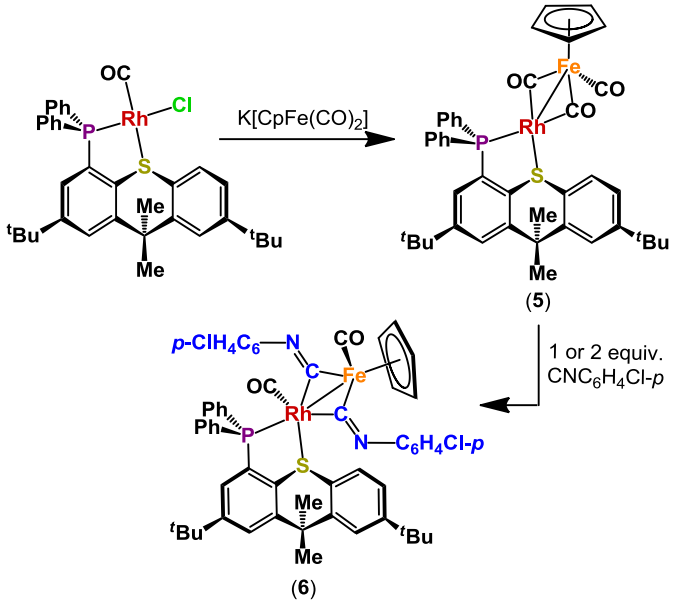

Complexes **5** and **6** gave rise to doublets at 45 and 44 ppm in their ^{31}P NMR spectra ($^{1}J_{P,Rh}$ 183 and 178 Hz, respectively). In the ^{13}C NMR spectrum of **5**, the CO ligand on iron and the bridging CO ligands appear as a broad singlet at 245.7 ppm, indicative of rapid exchange.[30] For compound **6**, the CO ligand on iron appears at 215 ppm, a peak at 202 ppm is tentatively assigned to the terminal CO ligand on rhodium, and the inequivalent bridging isonitrile ligands are assigned to signals at 248 and 242 ppm. For these quaternary signals, coupling was not observed due to low solubility (which resulted in low signal to noise even after 10,000 scans in a uDEFT experiment) and perhaps some residual fluxionality at –80 °C. However, the *C*NR signals for **6** are clearly at much lower frequency than the *C*NR signals for **2**-**4**, and fall within the range observed for related μ-isonitrile complexes (*vide supra*). Furthermore, the C–N stretching frequency for **6** is 1661 cm^{-1} (broad), which is 124 cm^{-1} higher than the C–N stretching frequency for **2**, highlighting the extent to which the C–N bond order is reduced in TXPB complex **2** relative to borane-free **6**.

X-ray quality crystals of **5**·2$C_2H_4Cl_2$ were grown from 1,2-dichloroethane/hexanes at –30 °C. The structure of **5** is compositionally analogous to that of **1**, except that **1** features an η^3*(BCC)*-interaction between rhodium and the pendant borane, and this interaction is absent in borane-free **5** (Figure 7, Table 1). The effects of the borane unit in **1** are reflected in very different geometries at

rhodium. The phosphine, thioether and carbonyl ligands in **5** form a square plane. By contrast, in compound **1**, rhodium, one bridging carbonyl ligand [C(61)], the phosphine, and the centroid of the η^3*(BCC)*-coordinated arylborane ($Cent^{BCC}$) occupy a plane [P(1)–Rh(1)–C(61) = 111.4°; C(61)–Rh(1)–$Cent^{BCC}$ = 120.4°; P(1)–Rh(1)–$Cent^{BCC}$ = 126.5°], with the thioether and the other bridging carbonyl ligand [C(71)] in axial positions relative to this plane [S(1)–Rh(1)–C(71) = 169.7°]. The Rh–Fe and Rh–P distances in TXPH complex **5** are also significantly shorter than those in **1**, likely as a consequence of greater steric hindrance and the geometric constraints of the TXPB ligand in compound **1**.

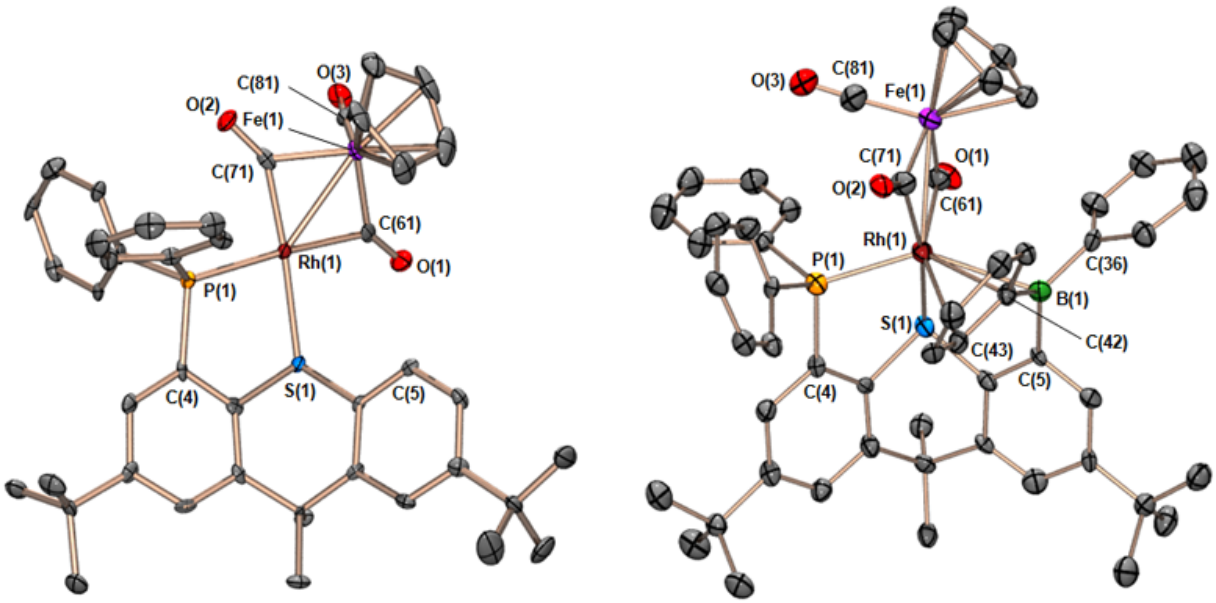

Figure 7. X-ray crystal structures for **5**·$2C_2H_4Cl_2$ and previously reported **1**·solvent (disordered solvent contains ~ 6.5 carbon atoms).[2] Hydrogen atoms, and lattice solvent are omitted for clarity. Ellipsoids are set to 50 % in **5**·$2C_2H_4Cl_2$ and 30 % in **1**·solvent.

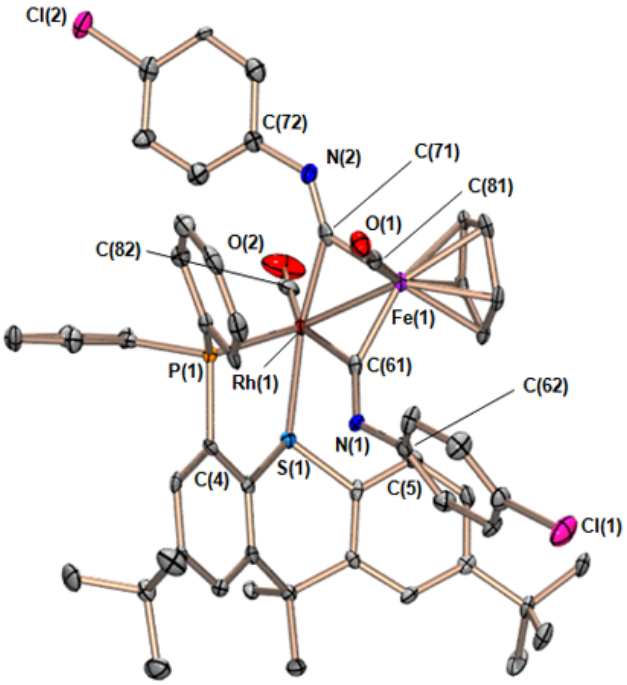

Figure 8. X-ray crystal structure for **6**·CH_2Cl_2. Hydrogen atoms and lattice solvent are omitted for clarity. Ellipsoids are set to 50 %.

X-ray quality crystals of **6**·CH_2Cl_2 were grown from dichloromethane/hexanes at –30 °C, and the structure features a κ^2-coordinated TXPH ligand on rhodium, a cyclopentadienyl ring on iron, a Rh–Fe distance of 2.631(1) Å, two bridging isonitrile ligands, and two terminal carbonyl ligands; one on iron and one on rhodium (Figure 8, Table 1). Excluding the Rh–Fe bond, the geometry at rhodium is distorted square pyramidal with the phosphine in the axial position; the S(1)–Rh(1)–C(71) angle is 171.7(1)°, while the C(61)–Rh(1)–C(82) angle is 154.5(2)°. Compared with TXPB complex **2**, the most distinct metrical features of **6** are: (a) elongated Fe–CNR bonds [1.908(5) and 1.943(5) Å in **6** versus 1.833(3) Å in **2**], (b) elongated Rh–CNR bonds [2.021(5) and 2.051(5) Å in **6** versus 1.968(3) Å in **2**], (c) shorter C–N distances [1.239(6) and 1.246(7) Å in **6** versus 1.284(3) Å in **2**], and (d) significantly more obtuse C–N–C angles [126.8(4)° and 132.7(4)° in **6** versus 117.5(2)° in **2**]. All features of **6** are unremarkable for a μ-isonitrile complex, and the structural and spectroscopic differences between **2** and

6 support the arguments for classification of the CNR(BR_3) unit in **2-4** as a μ-borataaminocarbyne ligand, rather than a borataazavinylidene ligand (a simple adduct between a borane and a μ-isonitrile ligand; see Figure 5).

Summary and Conclusions

Heterobimetallic **2-4**, [(TXPB)Rh(μ-CO)(μ-CNR)Fe(CO)Cp] (R = C_6H_4Cl-*p*, Xyl, ^nBu) were prepared in order to probe the nature of any interaction between a CNR ligand and a pendant borane. Isolated examples of transition metal complexes in which a Group 13 Lewis acid is bound to carbon monoxide or an isoelectronic neutral ligand are rare,[11,31] despite the potential for interactions of this type to greatly increase the thermodynamic favorability of 1,1-insertion reactions.[32] On the basis of their ^{13}C NMR data, C–N stretching frequencies, C–N and M–C bond distances, C–N–C angles, and comparison with a borane-free rhodium-iron isonitrile complex, [(TXPH)Rh(CO)(*μ*-CNC_6H_4Cl-*p*)$_2$Fe(CO)Cp] (**6**), complexes **2-4** are assigned as borataaminocarbyne [C–NR(BR_3)] complexes with a double bond between iron and the carbyne carbon atom, rather than borataazavinylidene [C=NR(BR_3)] complexes. To the best of our knowledge, [{Ir(CNXyl)}$_2${μ-C–NXyl(BH_3)}$_2$(μ-dmpm)$_2$] is the only other example of a borataaminocarbyne complex.

Experimental Section

General Details. An argon-filled MBraun UNIlab glove box equipped with a −30 °C freezer was employed for the manipulation and storage of the TXPB and TXPH ligands, as well as their complexes, and reactions were performed on a double manifold high vacuum line using standard techniques.[33] A Fisher Scientific Ultrasonic FS-30 bath was used to sonicate reaction mixtures where indicated. Residual oxygen and moisture was removed from the argon stream by passage through an Oxisorb-W scrubber from Matheson Gas Products.

Anhydrous CH_2Cl_2 was purchased from Aldrich. Hexanes and toluene were initially dried and distilled at atmospheric pressure from CaH_2 and Na, respectively. Unless otherwise noted, all proteo solvents were stored over an appropriate drying agent (toluene, benzene = Na/Ph_2CO; hexanes = Na/Ph_2CO/tetraglyme; CH_2Cl_2 = CaH_2) and introduced to reactions via vacuum transfer with condensation at −78 °C. Deuterated solvents (ACP Chemicals) were dried over CaH_2 (CD_2Cl_2) or Na/Ph_2CO (C_6D_6). CNC_6H_4Cl-*p*, CNXyl and CN^nBu were purchased from Sigma-Aldrich and stored under argon.

The TXPB ligand,[4] the TXPH ligand,[6] [RhCl(CO)(TXPB)],[2] [(TXPB)Rh(μ-$CO)_2$Fe(CO)Cp],[2] [RhCl(CO)(TXPH)],[6] K[$CpFe(CO)_2$][34] and $ClP(C_6D_5)_2$[35] [which was prepared from $Cl_2P(NEt_2)$][36] were prepared according to literature procedures. To assist in the complete assignment of the ^1H and ^{13}C NMR spectra for complexes **2-6**, the d_{10}-TXPB ligand, the d_{10}-TXPH ligand, and complexes ***d*$_{10}$-2**, ***d*$_{10}$-3, *d*$_{10}$-5** and ***d*$_{10}$-6** were prepared, in which the diphenylphosphino moiety is perdeuterated. Deuterated ligands were prepared using procedures identical to those for TXPB and TXPH, but using $ClP(C_6D_5)_2$. Deuterated complexes were prepared using procedures identical to those for **2**, **3, 5** and **6**, but using and d_{10}-TXPB and d_{10}-TXPH.

IR Spectra were recorded on a Thermo Scientific Nicolet 6700 FTIR spectrometer. Combustion elemental analyses were performed on a Thermo EA1112 CHNS/O analyzer. NMR spectroscopy (^1H, $^{13}C\{^1H\}$, ^{11}B, ^{19}F, ^{31}P, DEPT-135, uDEFT, COSY, TOCSY, HSQC, HMBC) was performed on Bruker DRX-500 and AV-600 spectrometers. All ^1H NMR and ^{13}C NMR spectra were referenced relative to $SiMe_4$ through a resonance of the employed deuterated solvent or proteo impurity of the solvent; C_6D_6 (7.16 ppm) and CD_2Cl_2 (5.32 ppm) for ^1H NMR; C_6D_6 (128.0 ppm) and CD_2Cl_2 (54.0 ppm) for ^{13}C NMR. ^{11}B, ^{31}P, and ^{19}F NMR spectra were referenced using an external standard of $BF_3(OEt_2)$ (0.0 ppm), 85% H_3PO_4 in D_2O (0.0 ppm), and $CFCl_3$ (0.0 ppm), respectively. Temperature calibration was performed using a d_4-methanol sample, as outlined in the Bruker VTU user manual. Herein, numbered proton and carbon atoms refer to the positions of the thioxanthene backbone in the TXPB and TXPH ligands.[6] Inequivalent phenyl rings on boron and carbon are labeled A and B so that the proton and

carbon resonances belonging to a single phenyl ring can be identified. We did not identify which *P*-phenyl ring gives rise to the signals labeled A or B, however the signals corresponding to the η^2-coordinated *B*-phenyl ring are labeled as B in complexes **2**-**4**.

X-ray crystallographic analyses were performed on suitable crystals coated in Paratone oil and mounted on a SMART APEX II diffractometer with a 3 kW Sealed tube Mo generator in the McMaster Analytical X-Ray (MAX) Diffraction Facility. In all cases, non-hydrogen atoms were refined anisotropically and hydrogen atoms were generated in ideal positions and then updated with each cycle of refinement. The following groups were rotationally or positionally disordered over two positions: (a) one of the *tert*-butyl substituents in **2**·2hexane, (b) both *P*-phenyl groups in **4**·2hexane, (c) one of the *B*-phenyl groups in **4**·2hexane, (d) the Cp-ring bound to iron in **4**·2hexane, (e) the bridging carbonyl group in **4**·2hexane, and (f) both molecules of 1,2-$C_2H_4Cl_2$ in **5**·$2C_2H_4Cl_2$. In addition, one molecule of hexane in **2**·2hexane, one molecule of toluene in **3**·5toluene and both molecules of hexane in **4**·2hexane were SQUEEZED from the lattice of each respective structure due to unresolveable disorder.[37] In all cases, disorder was modeled allowing occupancy and positional parameters to refine freely. *tert*-Butyl methyl groups (case (a) above) were restrained to have equivalent thermal parameters, and were refined anisotropically. For case (a), the *tert*-butyl group exhibited rotational disorder over two positions in a 72:28 ratio. For cases (b)–(d), phenyl ring and Cp ring carbon atoms were restrained to have similar thermal parameters through the use of the SIMU command. In terms of treatment of the *P*-phenyl groups in **4**·2hexane (case b), one of the *P*-phenyl groups (C24-C29) is positionally disordered in a 52:48 ratio over two positions, while the other (C30-C35) is positionally disordered over two positions in a 51:49 ratio. For case (c), one of the *B*-phenyl rings (C36-C41) is positionally disordered over two positions in a 51:49 ratio. In addition, the positional disorder within the Cp ring bound to iron (case d) was modeled in a 52:48 ratio over two positions. For case (e), the carbonyl ligand bridging between rhodium and iron was positionally disordered over two positions. The carbon atom of the carbonyl was modeled to have the same positional and thermal parameters for both positions, while the positional and thermal parameters of the oxygen atom were allowed to refine freely; the oxygen atom was found to be

positionally disordered in a 51:49 ratio. The carbon–chlorine bond distances in both molecules of solvent in **5**·2$C_2H_4Cl_2$ (case f) were restrained to approximately 1.77 Å. Anisotropic refinement of one of the molecules of 1,2-$C_2H_4Cl_2$ (C60, C61, Cl1, Cl2) resulted in unstable refinement of the carbon and chlorine atoms, therefore it was refined using the ISOR command. In addition, this molecule of solvent was positionally disordered in a 58:42 ratio over two positions, and its carbon atoms were refined to have the same thermal parameters. The other molecule of 1,2-$C_2H_4Cl_2$ (C70, C71, Cl3, Cl4) was refined anisotropically, but the carbon atoms and chlorine atoms were restrained to have similar thermal parameters through the use of the SIMU command, respectively. This molecule of solvent was positionally disordered over two positions in a 53:47 ratio.

[(TXPB)Rh(*μ*-CO)(*μ*-CNC$_6$H$_4$Cl-*p*)Fe(CO)Cp] (2): CNC_6H_4Cl-*p* (18 mg, 1.3 × 10^{-4} mol) dissolved in CH_2Cl_2 (3 mL) was added dropwise at RT to [(TXPB)Rh(μ-CO)$_2$Fe(CO)Cp]·0.6hexane (146 mg, 1.4 × 10^{-4} mol) in CH_2Cl_2 (8 mL). The reaction mixture was stirred vigorously for 30 min at RT before evaporating to dryness *in vacuo*. The resulting black/purple powder was dissolved in hexanes and cooled to –30°C overnight, after which time the hexane mother liquors were decanted and the dark purple crystals were dried *in vacuo*. Yield = 145 mg (94 %). X-ray quality crystals of **2**·2hexane were grown by cooling a saturated solution of **2** in hexanes to –30°C for several days. **^{1}H NMR (CD_2Cl_2, 194 K):** δ 7.69 (s, 1H, C*H*^{1}), 7.59 (s, 1H, C*H*^{8}), 7.43–7.30 (m, 8H, *m*-PhCl, *m*+*p*-P*Ph*$_2$ A, *m*+*p*-P*Ph*$_2$ B,), 7.30–7.20 (m, 5H, *o*-PhCl, *o*-P*Ph*$_2$ B, C*H*^{3}), 7.14 (s, 1H, C*H*^{6}), 6.99 (t, $^3J_{H,P}$ 9 Hz, 2H, *o*-P*Ph*$_2$ A), 6.82–6.73 (m, 5H, *o, m, p*-B*Ph*$_2$ A), 6.49 (t, $^3J_{H,H}$ 7 Hz, 1H, *m*-B*Ph*$_2$ B), 6.16 (d, $^3J_{H,H}$ 7 Hz, 1H, *o*-B*Ph*$_2$ B), 5.88 (t, $^3J_{H,H}$ 7 Hz, 1H, *m*-B*Ph*$_2$ B), 5.83 (d, $^3J_{H,H}$ 7 Hz, 1H, *o*-B*Ph*$_2$ B), 5.37 (t, $^3J_{H,H}$ 7 Hz, 1H, *p*-B*Ph*$_2$ B), 4.60 (s, 5H, C_5H_5), 2.16, 1.72 (br s, 2 x 3H, C*Me*$_2$), 1.16, 1.09 (s, 2 x 9H, C*Me*$_3$). **^{13}C{^{1}H} NMR (CD_2Cl_2, 298 K, selected data only):** δ 312.4 (dd, $^1J_{C,Rh}$ 53, $^2J_{C,P}$ 24 Hz, *μ*-*C*N(C$_6$H$_4$Cl-*p*)), 239.6 (dd, $^1J_{C,Rh}$ 56, $^2J_{C,P}$ 8 Hz, *μ*-*C*O), 216.3 (s, Fe-*C*O). **^{13}C{^{1}H} NMR (CD_2Cl_2, 194 K):** δ 312.4 (dd, $^1J_{C,Rh}$ 53, $^2J_{C,P}$ 24 Hz, *μ*-*C*N(C$_6$H$_4$Cl-*p*)), 241.9 (dd, $^1J_{C,Rh}$ 60, $^2J_{C,P}$ 10 Hz, *μ*-*C*O), 215.1 (s, Fe-*C*O), 150.6 (s, *C*^{2}CMe$_3$), 149.2 (s, *p*-PhCl), 148.9 (br s, *C*^{5}), 147.9 (s, *C*^{7}CMe$_3$), 146.4 (d, $^3J_{C,P}$ 11 Hz, *C*^{10}), 142.9 (s,

C^{13}), 137.7 (d, $^{2}J_{C,P}$ 34 Hz, *C*^{11}), 136.8 (d, $^{1}J_{C,P}$ 39 Hz, *ipso*-P*Ph*$_2$ B), 135.5 (br s, *ipso*-B*Ph*$_2$ A), 133.6 (s, *C*^{6}), 133.0 (br s, *ipso*-B*Ph*$_2$ B), 132.9 (d, $^{2}J_{C,P}$ 11 Hz, *o*-P*Ph*$_2$ A), 132.6 (d, $^{1}J_{C,P}$ 38 Hz, *C*^{4}), 132.6 (d, $^{2}J_{C,P}$ 14 Hz, *o*-P*Ph*$_2$ B), 132.4 (s, *C*^{12}), 130.8 (s, *ipso*-PhCl), 129.9 (s, *p*-P*Ph*$_2$ A), 129.6 (s, *o*-B*Ph*$_2$ B), 129.1 (s, *p*-P*Ph*$_2$ B), 128.8 (appt. s, *C*^{3}), 128.8 (s, *m*-PhCl), 128.1 (d, $^{3}J_{C,P}$ 10 Hz, *m*-P*Ph*$_2$ B), 127.6 (s, *p*-B*Ph*$_2$ A), 127.5 (d, $^{3}J_{C,P}$ 9 Hz, *m*-P*Ph*$_2$ A), 127 (d, *ipso*-P*Ph*$_2$ A), 126.5 (s, *m*-B*Ph*$_2$ B), 126.0 (br s, *o*-PhCl), 125.8 (s, *m*-B*Ph*$_2$ B), 125.2 (br s, *m*-B*Ph*$_2$ A), 124.5 (s, *p*-B*Ph*$_2$ B), 124.4 (s, *C*^{1}), 124.0 (s, *o*-B*Ph*$_2$ A), 121.0 (s, *C*^{8}), 115.7 (s, *o*-B*Ph*$_2$ B), 83.7 (s, *C*$_5$H$_5$), 42.7 (s, *C*Me$_2$), 34.7, 34.6 (s, 2 x *C*Me$_3$), 30.8, 30.6 (s, 2 x C*Me*$_3$), 25.4, 24.3 (s, 2 x C*Me*$_2$). **^{31}P{^{1}H} (CD$_2$Cl$_2$, 298 K):** δ 45.3 (d, $^{1}J_{P,Rh}$ 149 Hz). **^{11}B NMR (CD$_2$Cl$_2$, 298 K):** δ 4 (br s, $\omega_{1/2}$ 880 Hz). **IR** (nujol, ν/cm^{-1}): 1961, 1815 (CO), 1536 (CN). **IR** (CH$_2$Cl$_2$, ν/cm^{-1}): 1962, 1805 (CO), 1537 (CN). **Anal. Calcd.** For C$_{61}$H$_{57}$O$_2$NClBPSRhFe: C, 66.35; H, 5.20; N, 1.27%. **Found:** C, 66.90; H, 5.55; N, 1.03%.

[(TXPB)Rh(*μ*-CO)(*μ*-CNXyl)Fe(CO)Cp] (3): CNXyl (12 mg, 9.3 × 10^{-5} mol) dissolved in CH$_2$Cl$_2$ (3 mL) was added dropwise at rt to [(TXPB)Rh(μ-CO)$_2$Fe(CO)Cp]·0.6hexane (115 mg, 1.1 × 10^{-4} mol) in CH$_2$Cl$_2$ (10 mL). The reaction mixture was stirred vigorously for 30 min at rt before evaporating to dryness *in vacuo*. Yield = 92 mg (76 %). For further purification, the resulting black/red powder was dissolved in hexanes and cooled to –30°C overnight, after which time the hexane mother liquors were decanted and the resulting black needles were dried *in vacuo*. Yield = 59 mg (49 %). X-ray quality crystals of **3**·5toluene were grown by cooling a saturated solution of **3** in toluene to –30°C for several days. **^{1}H NMR (CD$_2$Cl$_2$, 194 K):** δ 7.68 (s, 1H, C*H*^{1}), 7.51 (s, 1H, C*H*^{8}), 7.42 (d, $^{3}J_{H,H}$ 7 Hz, 1H, *p*-P*Ph*$_2$ A), 7.38 (t, $^{3}J_{H,H}$ 7 Hz, 3H, *m*+*p*-P*Ph*$_2$ B), 7.32 (t, $^{3}J_{H,H}$ 7 Hz, 2H, *m*-P*Ph*$_2$ A), 7.28–7.25 (m, 2H, *o*-P*Ph*$_2$ A), 7.19 (d, $^{3}J_{H,P}$ 7 Hz, 1H, C*H*^{3}), 7.08 (d, $^{3}J_{H,H}$ 5 Hz, 2H, *m*-Xyl), 7.06 (s, 1H, *o*-B*Ph*$_2$ B), 7.03 (s, 1H, C*H*^{6}), 6.85 (t, $^{3}J_{H,H}$ 7 Hz, 1H, *o*-B*Ph*$_2$ A), 6.78 (br s, 1H, *p*-Xyl), 6.71 (t, $^{3}J_{H,H}$ 7 Hz, 1H, *m*-B*Ph*$_2$ A), 6.69 (t, $^{3}J_{H,H}$ 7 Hz, 1H, *m*-B*Ph*$_2$ A), 6.52–6.49 (m, 2H, *o*-B*Ph*$_2$ A + *m*-B*Ph*$_2$ B), 6.38 (d, $^{3}J_{H,H}$ 6 Hz, 1H, *o*-B*Ph*$_2$ B), 5.93 (t, $^{3}J_{H,H}$ 7 Hz, 1H, *m*-B*Ph*$_2$ B), 5.87 (d, $^{3}J_{H,H}$ 7 Hz, 1H, *o*-B*Ph*$_2$ B), 5.52 (d, $^{3}J_{H,H}$ 7 Hz, 1H, *p*-B*Ph*$_2$ A), 5.37 (t, $^{3}J_{H,H}$ 7 Hz, 1H, *p*-B*Ph*$_2$ B), 4.57 (s, 5H, C$_5$*H*$_5$), 2.34 (s, 3H, Xyl-C*H*$_3$), 2.14, 1.67

(s, 2 x 3H, C*Me*$_2$), 1.23 (s, 3H, Xyl-C*H*$_3$), 1.15, 1.04 (s, 2 x 9H, C*Me*$_3$). **^{13}C{^{1}H} NMR (CD_2Cl_2, 194 K):** δ 312.0 (dd, $^1J_{C,Rh}$ 52, $^2J_{C,P}$ 23 Hz, *μ-C*NXyl), 243.1 (dd, $^1J_{C,Rh}$ 60, $^2J_{C,P}$ 10 Hz, *μ-C*O), 215.5 (s, Fe-*C*O), 151.0 (br s, *ipso*-B*Ph*$_2$ A), 150.5 (s, *C*^{2}CMe$_3$), 150.0 (br s, *C*^{5}), 148.6 (s, *ipso*-Xyl), 147.9 (s, *C*^{7}CMe$_3$), 146.4 (d, $^3J_{C,P}$ 9 Hz, *C*^{10}), 142.4 (s, *C*^{13}), 138.0 (d, $^2J_{C,P}$ 34 Hz, *C*^{11}), 137.2 (d, $^1J_{C,P}$ 40 Hz, *ipso*-P*Ph*$_2$ A), 136.6 (s, *o*-B*Ph*$_2$ A), 135.0 (s, *p*-B*Ph*$_2$ A), 134.6 (s, *o*-Xyl), 134.0 (s, *C*^{12}), 133.5 (br s, *ipso*-B*Ph*$_2$ B), 133.0 (s, *C*^{6}), 132.9 (d, $^2J_{C,P}$ 12 Hz, *o*-P*Ph*$_2$ B), 132.8 (s, *o*-Xyl), 132.3 (d, $^2J_{C,P}$ 13 Hz, *o*-P*Ph*$_2$ A), 130.6 (d, $^1J_{C,P}$ 41 Hz, *C*^{4}), 130.0 (s, *o*-B*Ph*$_2$ B), 129.8 (s, *p*-P*Ph*$_2$ B), 129.1 (s, *p*-P*Ph*$_2$ A), 128.7 (s, *p*-Xyl), 128.7 (s, *C*^{3}), 128.1 (d, $^3J_{C,P}$ 9 Hz, *m*-P*Ph*$_2$ A), 127.8 (s, *m*-Xyl), 127.5 (d, $^3J_{C,P}$ 9 Hz, *m*-P*Ph*$_2$ B), 127 (d, *ipso*-P*Ph*$_2$ B), 126.7 (s, *m*-B*Ph*$_2$ B), 126.1 (s, *m*-Xyl), 125.9 (s, *m*-B*Ph*$_2$ B), 125.9 (s, *m*-B*Ph*$_2$ A), 124.7 (s, *p*-B*Ph*$_2$ B), 124.4 (s, *C*^{1}), 124.1 (s, *o*-B*Ph*$_2$ A), 123.9 (s, *m*-B*Ph*$_2$ A), 120.4 (s, *C*^{8}), 114.7 (s, *o*-B*Ph*$_2$ B), 83.5 (s, *C*$_5$H$_5$), 42.5 (s, *C*Me$_2$), 34.8, 34.6 (s, 2 x *C*Me$_3$), 30.9, 30.7 (s, 2 x C*Me*$_3$), 26.2, 23.6 (s, 2 x C*Me*$_2$), 19.6, 17.6 (s, 2 x Xyl-*C*H$_3$). **^{31}P{^{1}H} (CD_2Cl_2, 298 K):** δ 47.3 (d, $^1J_{P,Rh}$ 148 Hz). **^{11}B NMR (CD_2Cl_2, 298 K):** δ 4 (br s, $\omega_{1/2}$ 840 Hz). **IR** (nujol, ν/cm^{-1}): 1965, 1953, 1795 (CO), 1523 (CN). **IR** (CH_2Cl_2, ν/cm^{-1}): 1961, 1798 (CO), 1521 (CN). **Anal. Calcd.** For $C_{63}H_{62}O_2NBPSRhFe$: C, 68.93; H, 5.69; N, 1.28%. **Found:** C, 69.13; H, 6.01; N, 1.17%.

[(TXPB)Rh(*μ*-CO)(*μ*-CN*^{n}*Bu)Fe(CO)Cp] (4): CN*^{n}*Bu (10 mg, 1.2 × 10^{-4} mol) dissolved in CH_2Cl_2 (2 mL) was added dropwise at RT to [(TXPB)Rh(μ-CO)$_2$Fe(CO)Cp]·0.6hexane (116 mg, 1.1 × 10^{-4} mol) in CH_2Cl_2 (10 mL). The reaction mixture was stirred vigorously for 30 min at RT before evaporating to dryness *in vacuo*, yielding a dark purple powder. Yield = 99 mg (86%). X-ray quality crystals of **4** were grown by cooling a saturated solution of **3** in hexane/pentane to –30°C for several days. **^{1}H NMR (CD_2Cl_2, 253 K):** δ 7.69 (s, 1H, C*H*^{1}), 7.62 (s, 1H, C*H*^{6}), 7.59 (s, 1H, C*H*^{8}), 7.39–7.34 (m, 4H, *m*+*p*-P*Ph*$_2$ B, *p*-P*Ph*$_2$ A), 7.30 (t, $^3J_{H,H}$ 8 Hz, 2H, *m*-P*Ph*$_2$ A), 7.25–7.21 (m, 3H, *o*-P*Ph*$_2$ A, C*H*^{3}), 7.08–7.02 (m, 4H, *m*-B*Ph*$_2$ A, *o*-P*Ph*$_2$ B), 6.97 (t, $^3J_{H,H}$ 8 Hz, 1H, *p*-B*Ph*$_2$ A), 6.91 (d, $^3J_{H,H}$ 8 Hz, 2H, *o*-B*Ph*$_2$ A), 6.46 (t, $^3J_{H,H}$ 7 Hz, 1H, *m*-B*Ph*$_2$ B), 5.99 (t, $^3J_{H,H}$ 5 Hz, 2H, *o*-B*Ph*$_2$ B), 5.85 (t, $^3J_{H,H}$ 7 Hz, 1H, *m*-B*Ph*$_2$ B), 5.57 (t, $^3J_{H,H}$ 7 Hz, 1H, *p*-B*Ph*$_2$ B), 4.85 (s, 5H, C$_5$*H*$_5$), 4.38 (dt, $^2J_{H,H}$ 11, $^3J_{H,H}$ 4 Hz, 1H, ^{n}Bu-C*H*$_2^{\alpha}$),

4.11 (dt, $^{2}J_{H,H}$ 12, $^{3}J_{H,H}$ 6 Hz, 1H, ^{n}Bu-CH_2^{α}) 2.14 (s, 3H, CMe_2), 1.87 (do, $^{3}J_{H,H}$ 5 Hz, 1H, ^{n}Bu-CH_2^{β}), 1.71 (s, 3H, CMe_2), 1.45 (do, $^{3}J_{H,H}$ 5 Hz, 1H, ^{n}Bu-CH_2^{β}), 1.34 (sept., $^{3}J_{H,H}$ 7 Hz, 2H, ^{n}Bu-CH_2^{γ}), 1.24, 1.18 (s, 2 × 9H, CMe_3), 0.78 (t, $^{3}J_{H,H}$ 7 Hz, 3H, ^{n}Bu-CH_3). **^{13}C{^{1}H} NMR (CD_2Cl_2, 253 K):** 304.3 (dd, $^{1}J_{C,Rh}$ 51, $^{2}J_{C,P}$ 24 Hz, μ-*C*N^{n}Bu), 241.6 (dd, $^{1}J_{C,Rh}$ 60, $^{2}J_{C,P}$ 11 Hz, μ-*C*O), 215.9 (s, Fe-*C*O), 153.1 (br s, *ipso*-B*Ph*$_2$ A), 151.0 (d, $^{3}J_{C,P}$ 4 Hz, C^2), 149.7 (br s, C^5), 148.4 (s, C^7), 146.8 (d, $^{3}J_{C,P}$ 11 Hz, C^{10}), 143.3 (s, C^{13}), 138.5 (d, $^{2}J_{C,P}$ 33 Hz, C^{11}), 138.0 (d, $^{1}J_{C,P}$ 39 Hz, *ipso*-P*Ph*$_2$ A), 135.3 (s, *o*-B*Ph*$_2$ A), 133.7 (d, $^{2}J_{C,P}$ 12 Hz, *o*-P*Ph*$_2$ B), 133.5 (s, C^6), 132.9 (s, C^{12}, *ipso*-B*Ph*$_2$ B), 132.4 (d, $^{2}J_{C,P}$ 14 Hz, *o*-P*Ph*$_2$ A), 131.7 (d, $^{1}J_{C,P}$ 40 Hz, C^4), 130.5 (s, *o*-B*Ph*$_2$ B), 129.8 (s, *p*-P*Ph*$_2$ A), 129.5 (s, *p*-P*Ph*$_2$ B), 129.3 (s, C^3), 129.2 (d, $^{1}J_{C,P}$ 32 Hz, *ipso*-P*Ph*$_2$ B), 128.4 (d, $^{2}J_{C,P}$ 10 Hz, *m*-P*Ph*$_2$ A), 127.9 (d, $^{2}J_{C,P}$ 9 Hz, *m*-P*Ph*$_2$ B), 126.7 (s, *m*-B*Ph*$_2$ A), 126.3, 126.0 (s, *m*-B*Ph*$_2$ B), 124.9 (s, *p*-B*Ph*$_2$ B), 124.7 (s, *p*-B*Ph*$_2$ A), 124.6 (s, C^1), 120.6 (s, C^8), 117.7 (br s, *o*-B*Ph*$_2$ B), 83.4 (s, C_5H_5), 62.5 (d, $^{3}J_{C,Rh}$ 3 Hz, ^{n}Bu-*C*H$_2^{\alpha}$), 43.0 (s, *C*Me$_2$), 35.2 (s, 2 × *C*Me$_3$), 32.7 (s, ^{n}Bu-*C*H$_2^{\beta}$), 31.5, 31.2 (s, 2 × C*Me*$_3$), 26.7, 25.1 (s, 2 × C*Me*$_2$), 20.9 (s, ^{n}Bu-*C*H$_2^{\gamma}$), 14.0 (s, ^{n}Bu-*C*H$_3$). **^{31}P{^{1}H} (CD_2Cl_2, 298 K):** δ 44.1 (d, $^{1}J_{P,Rh}$ 151 Hz). **^{11}B NMR (CD_2Cl_2, 298 K):** δ 2 (br s, $\omega_{1/2}$ ~ 615 Hz). **IR** (nujol, ν/cm^{-1}): 1963, 1809 (CO), 1571, 1560 (CN). **IR** (CH_2Cl_2, ν/cm^{-1}): 1958, 1802 (CO), 1572, 1561 (CN). **Anal. Calcd.** For $C_{59}H_{62}O_2NBPSRhFe$: C, 67.51; H, 5.95; N, 1.33%. **Found:** C, 68.12; H, 6.10; N, 1.46%.

[(TXPH)Rh(μ-CO)$_2$Fe(CO)Cp] (5): Toluene (25 mL) was added to a mixture of K[CpFe(CO)$_2$] (178 mg, 8.2 × 10^{-4} mol) and [RhCl(CO)(TXPH)] (283 mg, 4.1 × 10^{-4} mol) and was stirred vigorously for 1.5 h at RT. The cherry red reaction mixture was then filtered; the brown solid collected on the surface of the frit was washed with toluene (5 mL × 2). The filtrate was evaporated to dryness *in vacuo* to yield a red/brown oily solid, to which hexanes (30 mL) was added. The mixture was sonicated and filtered to collect an orange/brown powder. The collected product was washed with hexanes (5 mL × 2) and dried *in vacuo*. Yield = 266 mg (78 %). X-ray quality crystals of **4**·2$C_2H_4Cl_2$ were grown by slow diffusion of hexanes into a saturated solution of **4** in 1,2-dichloroethane at –30°C. **^{1}H NMR (C_6D_6, 298 K):** δ 8.53 (d, $^{3}J_{H,H}$ 8 Hz, 1H, CH^5), 7.76–7.72 (m, 4H, *o*-P*Ph*$_2$), 7.64 (dd, $^{3}J_{H,H}$ 7, $^{4}J_{H,H}$ 2 Hz, 1H, CH^3), 7.60

(t, $^{4}J_{H,H}$ 2 Hz, 1H, C*H*^{1}), 7.59 (d, $^{4}J_{H,H}$ 2 Hz, 1H, C*H*^{8}), 7.17 (dd, $^{3}J_{H,P}$ 8, $^{4}J_{H,H}$ 2 Hz, 1H, C*H*^{6}), 6.98–6.97 (m, 6H, *m*+*p*-P*Ph*$_2$), 4.57 (s, 5H, C$_5$*H*$_5$), 1.69 (s, 6H, C*Me*$_2$), 1.21, 1.06 (s, 2 x 9H, C*Me*$_3$). **^{13}C{^{1}H} NMR (C$_6$D$_6$, 298 K):** δ 245.7 (br s, 3 x *C*O), 151.8 (d, $^{3}J_{C,P}$ 3 Hz, *C*^{2}CMe$_3$), 151.5 (s, *C*^{7}CMe$_3$), 145.9 (d, $^{3}J_{C,P}$ 10 Hz, *C*^{10}), 144.0 (s, *C*^{13}), 141.1 (d, $^{2}J_{C,P}$ 37 Hz, *C*^{11}), 135.6 (d, $^{1}J_{C,P}$ 40 Hz, *C*^{4}), 135.2 (d, $^{1}J_{C,P}$ 38 Hz, *ipso*-P*Ph*$_2$), 134.1 (d, $^{2}J_{C,P}$ 14 Hz, *o*-P*Ph*$_2$), 131.2 (s, *C*^{5}), 130.3 (s, *p*-P*Ph*$_2$), 130.1 (s, *C*^{3}), 129.6 (d, $^{4}J_{C,P}$ 4 Hz, *C*^{12}), 129.0 (d, $^{3}J_{C,P}$ 10 Hz, *m*-P*Ph*$_2$), 124.8 (s, *C*^{6}), 124.5 (s, *C*^{1}), 122.5 (s, *C*^{8}), 87.0 (s, *C*$_5$H$_5$), 42.8 (s, *C*Me$_2$), 35.3, (s, 2 x *C*Me$_3$), 31.8, 31.6 (s, 2 x C*Me*$_3$), 25.8 (s, C*Me*$_2$). Note: in the ^{13}C{^{1}H} NMR of **5** in *d*$_8$-toluene at 230 K, the CO signal was broadened into the baseline, consistent with rapid exchange between the three CO environments. **^{31}P{^{1}H} (C$_6$D$_6$, 298 K):** δ 45.3 (d, $^{1}J_{P,Rh}$ 183 Hz). **IR** (nujol, ν/cm^{-1}): 1956, 1946, 1938, 1756, 1750, 1740 (CO). **IR** (CH$_2$Cl$_2$, ν/cm^{-1}): 1960, 1741 (CO). **Anal. Calcd.** For C$_{43}$H$_{44}$O$_3$PSRhFe: C, 62.18; H, 5.34%. **Found:** C, 62.26; H, 5.62%.

[(TXPH)Rh(CO)(*μ*-CNC$_6$H$_4$Cl-*p*)$_2$Fe(CO)Cp] · CH$_2$Cl$_2$ (6): CNC$_6$H$_4$Cl-*p* (25 mg, 1.8 × 10^{-4} mol) dissolved in CH$_2$Cl$_2$ (1 mL) was added dropwise at RT to [(TXPH)Rh(μ-CO)$_2$Fe(CO)Cp] (75 mg, 9.0 × 10^{-5} mol) in CH$_2$Cl$_2$ (3 mL). The reaction mixture was stirred vigorously for 15 min at RT. The black/yellow solution was then layered with hexanes (10 mL) and cooled to –30°C for several days, after which point the mother liquors were decanted and the resulting black crystals were dried *in vacuo*. Yield = 49 mg (51 %). X-ray quality crystals of **5**·CH$_2$Cl$_2$ were grown by slow diffusion of hexanes into a saturated solution of **5** in CH$_2$Cl$_2$ at –30°C. **^{1}H NMR (CD$_2$Cl$_2$, 194 K):** δ 7.74 (br s, 2H, *o*-P*Ph*$_2$ A), 7.69 (s, 1H, C*H*^{1}), 7.74 (s, 1H, C*H*^{8}), 7.51 (s, 1H, C*H*^{3}), 7.46–7.38 (m, 5H, C*H*^{6}, *m*+*p*-P*Ph*$_2$ A, *p*-P*Ph*$_2$ B), 7.36 (d, $^{3}J_{H,H}$ 7 Hz, 1H, C*H*^{5}), 7.20 (d, $^{3}J_{H,H}$ 7 Hz, 2H, *o*-PhCl A), 7.09 (t, $^{3}J_{H,H}$ 7 Hz, 2H, *m*-P*Ph*$_2$ B), 6.91 (d, $^{3}J_{H,H}$ 7 Hz, 2H, *o*-PhCl B), 6.87 (t, $^{3}J_{H,H}$ 8 Hz, 2H, *o*-P*Ph*$_2$ B), 6.66 (d, $^{3}J_{H,H}$ 7 Hz, 2H, *m*-PhCl A), 5.60 (d, $^{3}J_{H,H}$ 7 Hz, 2H, *m*-PhCl B), 4.64 (s, 5H, C$_5$*H*$_5$), 2.10, 1.43 (s, 2 x 3H, C*Me*$_2$), 1.38, 1.19 (s, 2 x 9H, C*Me*$_3$). **^{13}C{^{1}H} NMR (CD$_2$Cl$_2$, 194 K):** δ 247.5, 242.3 (2 x br s, *μ*-*C*N(C$_6$H$_4$Cl-*p*)), 214.9 (s, Fe-*C*O), 202.1 (br d, $^{1}J_{C,Rh}$ 60 Hz, Rh-*C*O), 150.9 (s, *C*^{7}CMe$_3$), 149.7 (s, *C*^{2}CMe$_3$), 149.2 (s, *p*-PhCl A), 148.4 (s, *p*-PhCl B), 144.3 (d, $^{3}J_{C,P}$ 9 Hz, *C*^{10}), 144.0 (s, *C*^{13}), 138.3 (appt. s, *C*^{11}), 135.9 (d,

$^{1}J_{C,P}$ 32 Hz, *ipso*-P*Ph*$_2$ B), 133.9 (d, $^{1}J_{C,P}$ 32 Hz, *ipso*-P*Ph*$_2$ A), 132.9 (d, $^{2}J_{C,P}$ 14 Hz, *o*-P*Ph*$_2$ A), 131.8 (d, $^{1}J_{C,P}$ 39 Hz, C^4), 130.5 (s, C^3), 130.2 (d, $^{2}J_{C,P}$ 10 Hz, *o*-PPh$_2$ B), 129.9 (s, *p*-P*Ph*$_2$ A + B), 128.6 (s, C^5), 128.5 (s, *o*-PhCl A), 128.4 (d, $^{3}J_{C,P}$ 10 Hz, *m*-P*Ph*$_2$ A), 128.2 (s, *o*-PhCl B), 128.1 (s, C^{12}), 127.4 (d, $^{3}J_{C,P}$ 8 Hz, *m*-P*Ph*$_2$ B), 126.9 (s, *ipso*-PhCl A), 126.5 (s, *ipso*-PhCl B), 123.6 (s, C^1), 123.2 (s, C^6), 121.6 (s, C^8 + *m*-PhCl A), 120.0 (s, *m*-PhCl B), 82.3 (s, C_5H_5), 41.5 (s, *C*Me$_2$), 34.9, 34.8 (s, 2 x *C*Me$_3$), 31.2, 30.7 (s, 2 x C*Me*$_3$), 25.8, 24.8 (s, 2 x C*Me*$_2$). **^{31}P{^{1}H} (CD_2Cl_2, 298 K):** δ 43.7 (d, $^{1}J_{P,Rh}$ 178 Hz). **IR** (nujol, ν/cm^{-1}): 1950 (br, CO), 1659 (br, CN). **IR** (CH_2Cl_2, ν/cm^{-1}): 1954 (br, CO), 1661 (br, CN). **Anal. Calcd.** For $C_{57}H_{54}O_2N_2Cl_4PSRhFe$: C, 58.88; H, 4.68; N, 2.41%. **Found:** C, 59.02; H, 4.64; N, 2.14%.

ASSOCIATED CONTENT

Supporting Information. The X-ray crystal structure for **3**·5toluene, and tables of crystal data and structure refinement details for **2-6**. CIF files for **2-6** are available free of charge *via* the internet at http://pubs.acs.org.

AUTHOR INFORMATION

Corresponding Author

* Phone: 905-525-9140, Fax: 905-522-2509. E-mail: emslied@mcmaster.ca.

ACKNOWLEDGMENT

D.J.H.E. thanks NSERC of Canada for a Discovery Grant and B.E.C. thanks the Government of Canada for an NSERC PGS-D scholarship.

REFERENCES

(1) Emslie, D. J. H.; Cowie, B. E.; Kolpin, K. B. *Dalton Trans.* **2012**, *41*, 1101.

(2) Oakley, S. R.; Parker, K. D.; Emslie, D. J. H.; Vargas-Baca, I.; Robertson, C. M.; Harrington, L. E.; Britten, J. F. *Organometallics* **2006**, *25*, 5835.

(3) Emslie, D. J. H.; Harrington, L. E.; Jenkins, H. A.; Robertson, C. M.; Britten, J. F. *Organometallics* **2008**, *27*, 5317.

(4) Emslie, D. J. H.; Blackwell, J. M.; Britten, J. F.; Harrington, L. E. *Organometallics* **2006**, *25*, 2412.

(5) (a) Hill, A. F.; Owen, G. R.; White, A. J. P.; Williams, D. J. *Angew. Chem. Int. Ed.* **1999**, *38*, 2759. (b) Amgoune, A.; Bourissou, D. *Chem. Commun.* **2011**, 859. (c) Bouhadir, G.; Amgoune, A.; Bourissou, D. *Adv. Organomet. Chem.* **2010**, *58*, 1. (d) Sircoglou, M.; Bontemps, S.; Mercy, M.; Saffon, N.; Takahashi, M.; Bouhadir, G.; Maron, L.; Bourissou, D. *Angew. Chem. Int. Ed.* **2007**, *46*, 8583.

(6) D. J. H. Emslie; B. E. Cowie; S. R. Oakley; N. L. Huk; H. A. Jenkins; L. E. Harrington; Britten, J. F. *Dalton Trans.* **2012**, *41*, 3523

(7) (a) Barybin, M. V.; Meyers, J. J., Jr.; Neal, B. M., Renaissance of Isocyanoarenes as Ligands in Low-Valent Organometallics. In *Isocyanide Chemistry*, Nenajdenko, V., Ed.; Wiley: Hoboken, 2012; Ch. 14, p 493. (b) Hahn, F. E. *Angew. Chem. Int. Ed. Engl.* **1993**, *32*, 650.

(8) Cronin, D. L.; Wilkinson, J. R.; Todd, L., J. *J. Magn. Resonance* **1975**, *17*, 353.

(9) (a) Yamamoto, Y. *Coord. Chem. Rev.* **1980**, *32*, 193. (b) Lazar, M.; Angelici, R. J., Isocyanide Binding Modes on Metal Surfaces and in Metal Complexes. In *Modern Surface Organometallic Chemistry*, Basset, J.-M.; Psaro, R.; Roberto, D.; Ugo, R., Eds.; Wiley-VCH: Weinheim, 2009; Ch. 13, p 513. (c) Vogler, A., Coordinated Isonitriles. In *Isonitrile Chemistry*, Ugi, I., Ed.; Academic Press: New York and London, 1971; Ch. 10, p 217.

(10) Fehlhammer, W. P.; Schrolkamp, S.; Sperber, W. *Inorg. Chim. Acta* **1993**, *212*, 207. Complex **A** was not identified as a Lewis acid substituted aminocarbyne complex in the paper, and was not drawn as shown in Figure 3. However, the data, especially ν(CN), supports this bonding description.

(11) Wu, J. X.; Fanwick, P. E.; Kubiak, C. P. *J. Am. Chem. Soc.* **1989**, *111*, 7812.

(12) Watanabe, T.; Kurogi, T.; Ishida, Y.; Kawaguchi, H. *Dalton Trans.* **2011**, *40*, 7701.

(13) Related niobium amidocarbyne complexes have also been reported: Caselli, A.; Solari, E.; Scopelliti, R.; Floriani, C. *J. Am. Chem. Soc.* **1999**, *121*, 8296.

(14) Albano, V. G.; Busetto, L.; Cassani, M. C.; Sabatino, P.; Schmitz, A.; Zanotti, V. *J. Chem. Soc. Dalton Trans.* **1995**, 2087.

(15) Knorr, M.; Strohmann, C. *Eur. J. Inorg. Chem.* **1998**, 495.

(16) Goswami, A.; Maier, C. R.; Pritzkow, H.; Siebert, W. *J. Organomet. Chem.* **2005**, *690*, 3251.

(17) Albano, V. G.; Bordoni, S.; Busetto, L.; Camiletti, C.; Monari, M.; Palazzi, A.; Prestopino, F.; Zanotti, V. *J. Chem. Soc. Dalton Trans.* **1997**, 4665.

(18) Pombeiro, A. J. L.; Guedes da Silva, M. F. C.; Michelin, R. A. *Coord. Chem. Rev.* **2001**, *218*, 43.

(19) For NMR and IR data, see Figure S42 of the supporting information.

(20) Lutz, M.; Haukka, M.; Pakkanen, T. A.; Gade, L. H. *Organometallics* **2001**, *20*, 2631.

(21) Fukumoto, K.; Sakai, A.; Oya, T.; Nakazawa, H. *Chem. Commun.* **2012**, *48*, 3809.

(22) Hunt, I. D.; Mills, O. S. *Acta Cryst.* **1977**, *B33*, 2432.

(23) Akita, M.; Kato, S.; Terada, M.; Masaki, Y.; Tanaka, M.; Moro-oka, Y. *Organometallics* **1997**, *16*, 2392.

(24) Werner, H.; Schwab, P.; Bleuel, E.; Mahr, N.; Windmüller, B.; Wolf, J. *Chem. Eur. J.* **2000**, *6*, 4461.

(25) Werner, H.; Schwab, P.; Bleuel, E.; Mahr, N.; Steinert, P.; Wolf, J. *Chem. Eur. J.* **1997**, *3*, 1375.

(26) Jones, W. D.; Duttweiler, R. P., Jr.; Feher, F. J. *Inorg. Chem.* **1990**, *29*, 1505.

(27) Herrmann, W. A.; Weber, C.; Ziegler, M. L.; Serhadli, O. *J. Organomet. Chem.* **1985**, *297*, 245.

(28) Esteruelas, M. A.; Lahoz, F. J.; Oñate, E.; Oro, L. A.; Rodríguez, L. *Organometallics* **1993**, *12*, 4219.

(29) Kiviniemi, S.; Nissinen, M.; Alaviuhkola, T.; Rissanen, K.; Pursiainen, J. *J. Chem. Soc. Perkin Trans. 2* **2001**, 2364.

(30) In order for the bridging CO ligands to appear equivalent in the room temperature ^{13}C NMR spectrum of **5**, a low energy pathway must exist for their exchange, perhaps via an intermediate with a tetrahedral arrangement of the phosphine, thioether and carbonyl ligands, or a pathway involving thioether dissociation.

(31) (a) Abdalla, J. A. B.; Riddlestone, I. M.; Tirfoin, R.; Phillips, N.; Bates, J. I.; Aldridge, S. *Chem. Commun.* **2013**, *49*, 5547. (b) Conway, A. J.; Gainsford, G. J.; Schrieke, R. R.; Smith, J. D. *J. Chem. Soc., Dalton Trans.* **1975**, 2499. (c) Burlitch, J. M.; Leonowicz, M. E.; Petersen, R. B.; Hughes, R. E. *Inorg. Chem.* **1979**, *18*, 1097. (d) McDade, C.; Gibson, V. C.; Santarsiero, B. D.; Bercaw, J. E. *Organometallics* **1988**, *7*, 1. (e) Baibich, I. M.; Parlier, A.; Rudler, H.; Fontanille, M.; Lucas, C.; Soum, A. *Journal of Molecular Catalysis* **1989**, *53*, 193.

(32) (a) Kubo, K.; Nakazawa, H.; Nakahara, S.; Yoshino, K.; Mizuta, T.; Miyoshi, K. *Organometallics* **2000**, *19*, 4932. (b) Miller, A. J. M.; Labinger, J. A.; Bercaw, J. E. *J. Am. Chem. Soc.* **2008**, *130*, 11874.

(33) Burger, B. J.; Bercaw, J. E., Vacuum Line Techniques for Handling Air-Sensitive Organometallic Compounds. In *Experimental Organometallic Chemistry - A Practicum in Synthesis and Characterization*, American Chemical Society: Washington D.C., 1987; Vol. 357, p 79.

(34) Plotkin, J. S.; Shore, S. G. *Inorg. Chem.* **1981**, *20*, 284.

(35) Yamashita, M.; Vicario, J. V. C.; Hartwig, J. F. *J. Am. Chem. Soc.* **2003**, *125*, 16347.

(36) Tollefson, M. B.; Li, J. J.; Beak, P. *J. Am. Chem. Soc.* **1996**, *118*, 9052.

(37) Sluis, P. V. D.; Spek, A. L. *Acta Crystallogr.* **1990**, *A46*, 194.

For Table of Contents Use Only

Borataaminocarbyne Complexes, [$L_2Rh(\mu\text{-}CO)\{\mu\text{-}C\text{–}NR(BR_3)\}Fe(CO)Cp$], Formed by Intramolecular Isonitrile–Borane Coordination

Bradley E. Cowie and David J. H. Emslie*

TOC Text: Reaction of [(TXPB)Rh(μ-CO)$_2$Fe(CO)Cp] (**1**; TXPB = a phosphine-thioether-borane ambiphilic ligand) with isonitriles afforded [(TXPB)Rh(μ-CO)(μ-CNR)Fe(CO)Cp] {R = C_6H_4Cl-*p* (**2**), Xyl (**3**) and ^{n}Bu (**4**)}, in which the borane is bound to the nitrogen atom of the isonitrile ligand. Heterobimetallic **2**-**4** could be described either as borataaminocarbyne [C–NR(BR$_3$)] or borataazavinylidene [C=NR(BR$_3$)] complexes. C–N stretching frequencies, ^{13}C NMR data, C–N and M–C bond distances, C–N–C angles, and a borane-free rhodium-iron isonitrile complex, [(TXPH)Rh(CO)(μ-CNC$_6$H$_4$Cl-*p*)$_2$Fe(CO)Cp] (**6**; TXPH = the borane-free analogue of TXPB), are discussed in the context of determining the most appropriate bonding description for **2**-**4**.

TOC Graphic: